Chemical Geology 286 (2011) 185–195

Contents lists available at ScienceDirect

Chemical Geology

journal homepage: www.elsevier.com/locate/chemgeo

Sulfur geochemistry and microbial sulfate reduction during low-temperature alteration of uplifted lower oceanic crust: Insights from ODP Hole 735B

Susan E. Alford [a,b], Jeffrey C. Alt [a,*], Wayne C. Shanks III [c]

[a] Department of Geological Sciences, The University of Michigan, 1100 North University, Ann Arbor MI 48109-1005 USA
[b] School of Natural Sciences, University of California at Merced, 5200 North Lake Road, Merced CA 95343 USA
[c] U. S. Geological Survey, Denver Federal Center, MS 973, Denver, Colorado 80225, USA

ARTICLE INFO

Article history:
Received 7 September 2010
Received in revised form 30 April 2011
Accepted 3 May 2011
Available online 24 May 2011

Editor: U. Brand

Keywords:
Sulfur isotopes
Hydrothermal systems
Mid-ocean ridges
Subsurface biosphere
Ocean Drilling Program
Hole 735B

ABSTRACT

Sulfide petrography plus whole rock contents and isotope ratios of sulfur were measured in a 1.5 km section of oceanic gabbros in order to understand the geochemistry of sulfur cycling during low-temperature seawater alteration of the lower oceanic crust, and to test whether microbial effects may be present. Most samples have low $SO_4/\Sigma S$ values (≤ 0.15), have retained igneous globules of pyrrhotite ± chalcopyrite ± pentlandite, and host secondary aggregates of pyrrhotite and pyrite laths in smectite ± iron-oxyhydroxide ± magnetite ± calcite pseudomorphs of olivine and clinopyroxene. Compared to fresh gabbro containing 100–1800 ppm sulfur our data indicate an overall addition of sulfide to the lower crust. Selection of samples altered only at temperatures ≤110 °C constrains microbial sulfate reduction as the only viable mechanism for the observed sulfide addition, which may have been enabled by the production of H_2 from oxidation of associated olivine and pyroxene. The wide range in $\delta^{34}S_{sulfide}$ values (−1.5 to +16.3‰) and variable additions of sulfide are explained by variable $\varepsilon_{sulfate\text{-}sulfide}$ under open system pathways, with a possible progression into closed system pathways. Some samples underwent oxidation related to seawater penetration along permeable fault horizons and have lost sulfur, have high $SO_4/\Sigma S$ (≥ 0.46) and variable $\delta^{34}S_{sulfide}$ (0.7 to 16.9‰). Negative $\delta^{34}S_{sulfate}$–$\delta^{34}S_{sulfide}$ values for the majority of samples indicate kinetic isotope fractionation during oxidation of sulfide minerals. Depth trends in sulfide–sulfur contents and sulfide mineral assemblages indicate a late-stage downward penetration of seawater into the lower 1 km of Hole 735B. Our results show that under appropriate temperature conditions, a subsurface biosphere can persist in the lower oceanic crust and alter its geochemistry.

1. Introduction

Reaction of seawater with oceanic crust results in significant chemical exchange, buffering the composition of seawater and affecting the geochemistry of the lithosphere entering subduction zones (Edmond et al., 1979a; Zindler and Hart, 1986; Wheat and Mottl, 2000; Boschi et al., 2008; Shilobreeva et al., 2011). Fluid–rock interaction also supports chemosynthetically based biological communities on and beneath the seafloor that can impose further chemical changes on seawater and crustal reservoirs (Edwards et al., 2004, 2005). In particular, sulfur geochemistry varies with temperature and redox, and is affected by kinetic and biological effects, making sulfur a good tracer of hydrothermal and microbial processes (e.g., Alt and Shanks, 1998, 2003; Alt et al., 2003, 2007; Delacour et al., 2008a,b; Rouxel et al., 2008).

Active high-temperature hydrothermal systems at mid-ocean ridges are driven by magmatic heat sources at depth, and vent hydrothermal fluids at the seafloor to form spectacular black smokers and massive sulfide deposits (Edmond et al., 1979a,b). Mixing of these acidic, reducing, and metal-rich fluids with seawater supports microbial communities on and within chimney vent structures, on the seafloor, and in the shallow subsurface around hydrothermal vents (see summary in Kelley et al., 2002). At temperatures of ~150 °C down to near 0 °C, circulation of fluids in the upper few hundred meters of volcanic basement on ridge flanks and in the ocean basins progresses as passive hydrothermal circulation, driven by cooling of the oceanic lithosphere (Fisher, 1998). Water–rock interactions in these systems also produce important chemical changes, and support a vast subsurface biosphere in oceanic basement (Fisk et al., 1998; Torsvik et al., 1998; Furnes and Staudigel, 1999; Alt et al., 2003; Bach and Edwards, 2003; Cowen et al., 2003; Huber et al., 2006). Open circulation of cold oxygenated seawater in these passive environments leads to the breakdown and oxidation of sulfide minerals, and loss of sulfur from basement rocks (Alt, 2004). Where basement is sealed to seawater by overlying sediment, more restricted circulation and reducing conditions prevail, and pyrite is a common secondary mineral in altered basalts (Honnorez, 2003). The very slow reaction kinetics of sulfate at the low temperatures (<100 °C) and moderate

* Corresponding author. Fax: +1 734 763 4690.
E-mail addresses: salford@ucmerced.edu (S.E. Alford), jalt@umich.edu (J.C. Alt), pshanks@usgs.gov (W.C. Shanks).

0009-2541/$ – see front matter © 2011 Elsevier B.V. All rights reserved.
doi:10.1016/j.chemgeo.2011.05.005

pH (~6) of these systems precludes inorganic reactions for pyrite formation (Malinin and Khitarov, 1969; Seyfried and Bischoff, 1979; Ohmoto and Lasaga, 1982; Goldstein and Aizenshtat, 1994; Ohmoto and Goldhaber, 1997; Alt, 2004). Sulfur isotope data for basement volcanic rocks provide evidence for microbially mediated reduction of seawater sulfate as the mechanism for this local addition of sulfur to the upper oceanic crust (Alt et al., 2003; Rouxel et al., 2008). Based on modeling of seawater entrainment and fluid flow within ridge flanks, such biologically mediated reactions in the volcanic upper crustal environments of ridge-flanks may persist for tens of Mya (Hutnak et al., 2008).

On slow spreading ridges, lower crustal gabbros and upper mantle peridotites are commonly exposed at the seafloor in oceanic core complexes consisting of a core of relatively unaltered gabbro within either highly deformed gabbro or serpentinized peridotite occurring as topographic highs at inside-corners of ridge-transform intersections (Tucholke et al., 1998; Carbotte and Scheirer, 2004; Buck et al., 2005). The exposure of these lower crustal rocks occurs as the result of episodic emplacement of magmas in concert with continual extension of the lithosphere, allowing for the formation of a heterogeneous "plum-pudding" architecture of the lower crust and the formation of low-angle detachment faults (Carbotte and Scheirer, 2004; Buck et al., 2005; Ildefonse et al., 2007). During uplift, formation of brittle faults and infiltration of seawater leads to late-stage alteration of the outer portions of the uplifted block, as well as localized areas of the gabbroic core from amphibolite facies conditions down to low temperatures (Karson, 1998; Escartin et al., 2003; Ildefonse et al., 2007). The low-temperature alteration of peridotite exposed in these environments commonly supports microbial activity, in particular sulfate reducers, adding isotopically fractionated sulfide to the rocks (Alt and Shanks, 1998; Alt et al., 2007; Delacour et al., 2008a). Studies of oceanic gabbros have yet to show similar evidence for microbial sulfate reduction, however the gabbros investigated in previous studies were mainly affected by higher-temperature hydrothermal alteration and were subjected to only minimal low-temperature seawater–rock interaction (Alt et al., 2007; Delacour et al., 2008b).

ODP Hole 735B in the SW Indian Ocean penetrates a 1.5 km section of lower crustal gabbros, which were locally affected by brittle fracturing and low-temperature (down to 10 °C) late-stage alteration (Dick et al., 2000; Alt and Bach, 2001; Bach et al., 2001). This paper presents the results of an investigation of the geochemistry of sulfur in Hole 735B gabbros, with the goal of examining evidence for microbial sulfate reduction during low-temperature alteration of exposed lower oceanic crust. We present sulfide mineral petrography and analyses of the contents and isotopic composition of sulfur in these rocks. Results indicate that microbial sulfate reduction was an important process, and suggest that oxidation of sulfide minerals was related to penetration of oxidizing seawater along permeable fault horizons.

2. Geological setting of site 735

ODP Site 735 is located on Atlantis Bank, an exposure of lower oceanic crustal material near the top of a transverse ridge along the Atlantis II Fracture Zone at 32°43.392'S, 57°15.960'E (Fig. 1). This portion of crust formed at the ultra-slow spreading Southwest Indian Ridge (SWIR) at 11.5 mya, and was exposed by detachment faulting at 11 mya as an oceanic core complex at the intersection of the paleo-SWIR and the Atlantis II Fracture Zone (John et al., 2004). Subsequent cooling of the detached block allowed for temperatures of <110 °C to be attained by 7 Ma, 4–5 m.y. off-axis (John et al., 2004). Hole 735B was drilled to a depth of ~500 m below seafloor (mbsf) on ODP Leg 118, and later extended to a final depth of 1508.0 mbsf during ODP Leg 176. Core recovery was extremely high for both Legs 118 and 176, averaging ~87% (Shipboard Scientific Party, 1999).

Hole 735B has been divided into 12 lithologic units, defined by grain size and primary modal mineralogy (Table 1). The applied classification scheme follows the International Union of Geological Sciences system with some modifications such that "disseminated oxide gabbros" contain 1 to 2% Fe–Ti oxides, "oxide gabbros" contain greater than 2% Fe–Ti oxides, "gabbronorites" contain >5% orthopyroxene and the modifier "troctolitic" defines gabbros with 5 to15% clinopyroxene. (Shipboard Scientific Party, 1999).

A series of events led to variations in the type and distribution of alteration effects with depth in Hole 735B (Shipboard Scientific Party, 1999). Initial dynamothermal metamorphism during exhumation of overlying crustal material resulted in high-temperature crystal–plastic deformation in zones of highly foliated rock, predominantly in the upper 200 m. Subsequent cooling and cracking allowed formation of brittle fractures and sub-vertical amphibole veins in the upper 700 m, and mediated high-temperature "static alteration" manifest as coronas of amphibole ± talc surrounding pyroxene and olivine. Later cooling and uplift of the ridge led to further fracturing and penetration of cold seawater, forming late-stage smectite, chlorite, carbonate, and zeolite ± prehnite veins throughout Hole 735B.

Alt and Anderson (1991) studied sulfur in the upper 500 m recovered on Leg 118, and showed: 1) a general loss of sulfur to hydrothermal fluids due to the breakdown of igneous sulfides during high-temperature (>350 °C) dynamothermal metamorphism; and 2) local oxidation by late-stage circulation of seawater. Lithologic unit IV

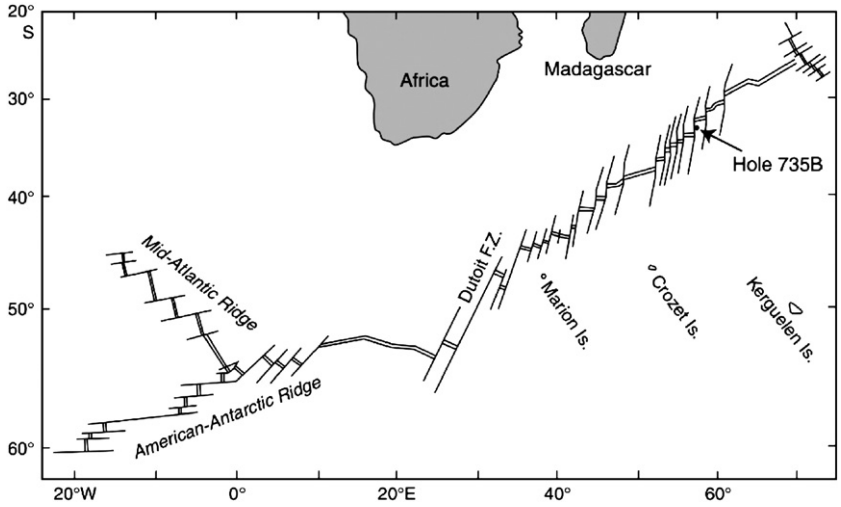

Fig. 1. Location of ODP Hole 735B in the SW Indian Ocean. (after Natland et al., 2002).

Table 1
Lithologic units of Hole 735B.

Drill Leg	Unit	Base of Unit		Lithology
		Hole-Leg-core-section-interval, cm	Depth* (mbsf)	
LEG 118	I	735B-118-10D-1, 70	37.41	Gabbronorite
	II	-35R-6, 72	170.22	Upper Compound Olivine Gabbro
	III	-46R-2, 150	223.57	Disseminated Oxide-Olivine Gabbro
	IV	-56R-3, 116	274.06	Massive Oxide Olivine Gabbro
	V	-74R-6, 3	382.40	Massive Olivine Gabbro
———	VI	-176-93R-5, 33	537.37	Lower Compound Olivine Gabbro
LEG 176	VII	-103R-3, 78	600.76	Gabbronorite & Oxide Gabbronorite
	VIII	-115R-6, 81	669.84	Olivine Gabbro
	IX	-120R-3, 142	714.35	Gabbronorite & Gabbro
	X	-149 R-1, 73	961.23	Olivine Gabbro & Gabbro
	XI	-188R-6, 14	1314.12	Olivine Gabbro
	XII	-210R-7, 142	1508.00	Olivine Gabbro & Troctolitic Gabbro

*Basal depth of lithologic units as presented by Dick et al., (1991) and Shipboard Scientific Party (1999).

within this upper 500 m is a highly evolved oxide olivine gabbro containing abundant Fe–Ti oxides, sulfide minerals, and high sulfur contents, as the result of igneous fractionation and concentration of sulfides and oxides (Alt and Anderson, 1991). Bach et al. (2001) divided the entire 1.5 km of Hole 735B into eight low-temperature alteration zones based on differences in secondary mineralogy and geochemistry between less-altered and more extensively altered samples (Table 2) (Bach et al., 2001). These authors showed that sulfur has been variably added and lost in different low-temperature alteration zones of Hole 735B.

3. Methods

3.1. Sample selection

Fifteen whole-rock samples from low-temperature alteration zones 1 through 5 and three pairs of highly and minimally altered whole-rocks from zone 2 were selected for study based on the presence of low temperature phases including iron-oxyhydroxides, calcite, smectite and zeolites, and the general absence of large (>300 μm) igneous sulfides. Oxygen isotope analyses of these phases indicate that they formed at temperatures less than about 110 °C, down to 10 °C (Alt and Bach, 2001). The paired samples are characterized by a host rock and a low-temperature alteration halo, which were separated into “minimally altered” and “highly altered” sub-samples, respectively. No samples were chosen from alteration zone 6 (1475–1508 mbsf), as this zone is characterized by greenschist-facies assemblages (Bach et al., 2001) and whole-rock ^{18}O depletions (Alt and Bach, 2006), indicating alteration temperatures in excess of 250 °C.

Table 2
Low-temperature alteration zones of Hole 735B.

Alteration Zone	Depth Range (mbsf)	Alteration Type	Chemical Changes
1'	0–40	Oxidative	+ ^{16}O
2'	40–500	Nonoxidative	+ ^{16}O
1	500–600	Oxidative	+ ^{18}O, C
2	600–835	Nonoxidative	+ C, ^{18}O, S
3	835–1050	Nonoxidative	–
4	1050–1300	Nonoxidative	+ C, ^{18}O, S
5	1300–1475	Nonoxidative	+ C, ^{18}O
6	1475–1508	Greenschist facies	+ ^{16}O

Adapted from (Bach et al., 2001).

3.2. Petrography and mineralogy

Each sample selected for analysis was examined in hand specimen and thin section under transmitted and reflected light to document petrogenic relationships. Eight samples representing alteration effects typical of different lithologic unit and alteration zone combinations were subsequently selected for compositional analysis of sulfide minerals on a CAMECA SX-100 Electron Microprobe Analyzer. Operating conditions were: 20 kV accelerating voltage; 20 nA sample current; 1 μm spot size.

3.3. Sample preparation and sulfur extractions

Sample surfaces were abraded with an aluminum oxide grinding wheel and air-blasted to remove any surface contamination. Samples were then broken in a steel jaw crusher, and powdered in a tungsten carbide shatterbox. All equipment was scrubbed with water, rinsed with 70% ethyl alcohol, and air-blasted between samples.

Powdered samples were dried overnight at 100 °C and stored in a dessicator under vacuum. Separate fractions of sulfur were extracted from ~9.5g of individual sample powders following Rice et al. (1993) and Tuttle et al. (1986). First, an acid-volatile sulfide (AVS) fraction was extracted by reaction of sample powders in 6 N HCl with $SnCl_2$ for 5 min under boiling conditions, followed by sub-boiling conditions for 30 min. After recovery of the AVS fraction, a chromium-reduced sulfide (CRS) fraction representative of mainly disulfides was extracted by using an acidified $CrCl_2$ solution (Zhabina and Volkov, 1978; Canfield et al., 1986) where contents of the reaction vessel were boiled for 1–2 h. The final digestion in the extraction procedure targeted sulfates by boiling the remaining contents in the reaction vessel for 2–3 h with a solution of $HCl + H_3PO_2 + HI$ modified from Thode et al. (1961). All digestions were carried out sequentially in a closed reaction vessel through which N_2 gas continuously flowed to serve as a carrier gas to transport evolved H_2S to a $AgNO_3$ precipitation trap and to maintain a reduced atmosphere in the system. The weight of the recovered Ag_2S precipitate was determined gravimetrically for each fraction.

3.4. Sulfur isotope analysis

The Ag_2S precipitates were analyzed for sulfur isotope composition at the United States Geological Survey stable isotope laboratory in Denver, Colorado. The precipitates were combusted to SO_2 with an elemental analyzer and introduced directly via continuous flow mode to a Micromass Optima mass spectrometer for measurement of $^{34}S/^{32}S$ ratios. Results are reported in standard δ-notation relative to Vienna Canyon Diablo Troilite (V-CDT) in per mil (‰), where the $\delta^{34}S$ of the synthetically produced silver sulfide standards IAEA-S-1 and IAEA-S-2 have been defined as −0.3‰ and 22.67‰ relative to V-CDT and the original CDT sulfur standard (Coplen and Krouse, 1998). Replicate measurements of standards were reproducible to ±0.2‰. Due to limits of detection, only Ag_2S precipitates that weighed at least 1 mg were analyzed. Use of the recently defined V-CDT scale is necessary due to depletion of the original CDT standard, and also allows for greater precision than what has been achievable using the naturally occurring heterogeneous CDT (Beaudoin et al., 1994).

4. Results

4.1. Sulfide petrography

Representative microprobe analyses of sulfide minerals are presented in Table 3. Two types of sulfide minerals were analyzed:

Table 3
Results of representative electron microprobe analyses from the Leg 176 section of Hole 735B.

Alt.Zone-Lith. Unit-	Core-Section, interval (cm)	Description	Elements (Wt %)					
			S	Fe	Co	Ni	Cu	Total
1-VII	99R-1, 113–118	CT-2-SM-V	28.39	4.33	0.01	––	57.04	89.76
		PY-1-SM-I	52.55	44.02	0.36	1.37	0.16	98.46
1-VIII	103R-4, 72–76	CP-2-CC-V	35.05	29.69	0.09	0.02	33.79	98.63
		G-1-SM-I	41.16	55.96	0.16	0.46	0.03	97.76
		PO-2-SM-ROL	39.86	59.30	0.12	0.06	0.03	99.37
2-IX	116R-3, 39–44	PY-2-CC-V	53.06	45.63	0.06	0.03	––	98.78
		PY-2-SM-V	53.16	46.20	0.07	0.01	––	99.43
		PY-2-FF-PL	53.06	45.87	0.06	––	0.01	99.01
		PY-2-FF-CPX	53.59	45.37	0.05	0.01	––	99.02
		PY-2-SM-RCPX	52.84	46.72	0.08	––	––	99.64
2-X	131R-1, 120–125	PY-2-SMT-ROL	52.29	46.23	0.17	0.13	0.01	98.84
		PY-2-SM-ROL	52.07	46.13	0.09	0.07	––	98.36
		PY-2-FX-ROL	51.95	46.18	0.08	0.08	––	98.29
		PO-2-FX-ROL	38.78	59.93	0.09	0.01	––	98.82
		PO-1-SM-I	38.50	59.84	0.09	0.01	0.03	98.48
		PN-1-SM-I	33.41	32.45	7.05	25.87	0.12	98.90
		CP-1-SM-I	34.60	30.27	0.09	0.02	33.01	97.98
3-X	140R-1, 119–124	PY-2-Z-V	51.87	45.83	0.06	––	0.01	97.77
		PO-2-SM-ROL	38.36	58.02	0.10	0.07	0.02	96.58
3-XI	159–2, 74–80	PY-2-FX-ROL	52.24	45.91	0.08	0.05	––	98.27
		PO-2-SM-OPX	39.10	57.75	0.13	0.05	0.19	97.21
		PO-2-FX-ROL	39.35	58.31	0.11	0.02	0.67	98.46
		PO-1-SM-I	39.60	59.19	0.10	0.14	0.03	99.05
		CP-1-SM-I	34.31	30.07	0.05	0.01	33.21	97.64
4-XI	177R-5, 61–66	CP-1-CC-I	37.06	29.45	0.04	0.10	33.74	100.38
		ID-1-CC-I	32.18	16.23	0.03	0.03	51.63	100.10
		XBN-1-CC-I	28.00	10.92	0.02	––	61.12	100.05
		PY-2-SM-V	56.32	46.36	0.08	––	––	102.76
		PN-1-SM-OL	35.01	28.41	2.11	35.41	0.16	101.11
		CP-1-SM-PL	37.10	29.97	0.04	––	33.86	100.97
		PO-1-SM-PL	40.94	59.30	0.10	0.04	0.68	101.05
		PN-1-SM-PL	35.09	33.74	2.82	29.59	0.06	101.29
		PO-2-SM-ROL	38.17	59.03	2.19	0.20	––	99.59
5-XII	196R-5, 126–133	PO-2-SM-ROL	38.28	61.83	0.10	0.01	––	100.22
		PO-2-CC-ROL	38.32	61.77	0.10	––	––	100.19
		CP-2-SM-ROL	35.98	30.20	0.04	0.01	33.65	99.88
		PN-2-SM-ROL	35.38	21.67	11.86	31.66	0.04	100.60
		CP-1-Z-I	37.59	29.46	0.06	0.05	33.04	100.20
		PN-1-Z-I	34.96	24.26	4.280	36.56	0.08	100.14
		CP-2-Z-RPL	36.61	29.52	0.04	––	33.54	99.71

*Description: analyzed sulfide mineral-alteration type-associated alteration mineral-occurrence where PY = pyrite, PO = pyrrhotite, PN = pentlandite, CT = chalcocite, CP = chalcopyrite, G = greigite, ID = idaite, XBN = anomalous bornite, 1 = primary, 2 = secondary, CC = calcite, FX = iron-oxyhydroxide, SM = smectite, SMT = smectite-talc, Z = zeolite, FF = fracture filling, ROL = replacing olivine, RCPX = replacing clinopyroxene, RPL = replacing plagioclase, OL = in olivine, PL = in plagioclase, CPX = in clinopyroxene, OPX = in orthopyroxene, V = vein, I = interstitial.

"igneous sulfides" and "secondary sulfides" based on mode of occurrence. Igneous sulfides are defined here as sulfide globules within igneous silicate grains or in interstitial areas, and may or may not be rimmed by alteration minerals. Secondary sulfides fill fractures or occur as sub- to euhedral grains within or replacing altered igneous silicates. None of the most common sulfide minerals, pyrite, pyrrhotite, pentlandite and chalcopyrite, are found exclusively as either igneous sulfide or secondary modes.

4.1.1. Igneous Sulfides

Igneous sulfides in alteration zones 2 through 5 commonly occur as monomineralic pyrrhotite or chalcopyrite, or as assemblages of pyrrhotite ± chalcopyrite ± pentlandite (Fig. 2; Table 3), and are commonly surrounded by rims of smectite, iron-oxyhydroxide or calcite. The mineralogy of the igneous sulfides is similar to that described previously for primary igneous sulfides in Hole 735B (Alt and Anderson, 1991; Miller and Cervantes, 2002). Rare ~100 μm subhedral grains displaying optical properties and chemical compositions approaching sulfur-rich x-bornite ($Cu_{4.610}Fe_{0.935}S_{4.05}(Co_{0.001})$) and idaite ($Cu_{3.345}Fe_{1.194}S_4(Co_{0.021})(Ni_{0.023})$) with lamellae of chalcopyrite were observed in interstitial calcite in sample 177R-5, 61–66 cm, and are most likely alteration products of primary igneous sulfides.

Alteration zone 1 is characterized by porous textures of sulfide minerals. The few igneous sulfides in this zone include rare ≤20 μm porous pyrite globules (99R-1, 113–118 cm), and rare ~20 × 55 μm anhedral greigite in interstitial smectite (103R-4, 72–76 cm). Such porous textures of sulfide minerals are generally absent in alteration zones 2–5, although rare ≤1 mm interstitial subhedral pyrite and pyrrhotite ± chalcopyrite grains displaying porous textures are present in sample 116R-3, 39–44 cm in zone 2. Secondary magnetite within pseudomorphs of olivine and clinopyroxene in alteration zone 1 is partly altered to hematite.

4.1.2. Secondary sulfides

The most common secondary sulfides in alteration zones 2 through 5 are part of an assemblage of smectite ± iron-oxyhydroxide ± calcite ± magnetite replacing olivine and clinopyroxene grains. This assemblage occurs as pseudomorphs of olivine and clinopyroxene within 1 cm of 0.5 to 2 mm wide veins of smectite ± calcite, or as a "mesh" texture among kernels of relict olivine and clinopyroxene in the host rock farther from the veins (Fig. 3a,b). In the host rock, aggregates of secondary pyrrhotite laths are concentrated linearly within fractures of the "mesh" texture and along the inside edge of pseudomorphs. The pyrrhotite laths commonly display a porous texture. In contrast, silicate pseudomorphs

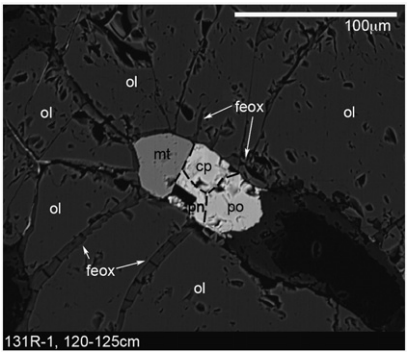

Fig. 2. BSE (back-scattered electron) image of igneous sulfide. cp = chalcopyrite, feox = iron oxyhydroxide, mt = magnetite, ol = olivine, po = pyrrhotite and pn = pentlandite. Dashed lines highlight grain boundaries.

in the wallrock close to the smectite ± calcite veins contain lath-shaped pyrite, suggesting that the pyrite has replaced pyrrhotite. In alteration zone 1, olivine and clinopyroxene replacements are abundant, but lack the associated secondary sulfide minerals common to alteration zones 2 through 5.

In addition to the presence of secondary sulfides in altered olivine and pyroxene, secondary sulfides also occur in major veins, interstitial areas, and fractures. Pyrite is the most common vein-associated secondary sulfide, present within calcite + smectite, smectite, and zeolite veins (Fig. 3c,d). The vein-associated pyrite is commonly present as ≤5 µm sub- to euhedral grains in minor amounts, however, a large calcite vein in sample 107R-1, 81–86 cm hosts ~100 µm pyrite grains. Pyrite also fills fractures and occurs as sub- to euhedral blocky grains in interstitial areas in alteration zone 2. Additional secondary sulfides are uncommon, but are present as rare ~6 to 110 µm porous chalcopyrite ± trace ≤5 µm globular chalcocite in smectite-lined calcite veins (Fig. 4a,b), and as trace sub- to euhedral 100 × 35 µm chalcopyrite ± ≤40 µm globular pentlandite in interstitial smectite.

4.2. Sulfur contents

Total sulfur contents of samples from this study range from 269 to 8305 ppm (Table 4), with the highest sulfur contents restricted to the low-temperature alteration zones 2 and 4 as defined by Bach et al. (2001) (Fig. 5). Total sulfide sulfur (AVS + CRS) ranges from 85 to 8187 ppm with an average of 1933 ppm, while sulfate sulfur ranges from 8 to 522 ppm with an average of 116 ppm. AVS contents range from ~0 (not detected) to 6123 ppm, with samples from alteration zone 4 encompassing nearly this full range whereas all other zones are limited to less than 1000 ppm AVS (Fig. 5). CRS ranges from 9 to 7564 ppm with alteration zones 2 and 4 containing widely varying CRS contents, while all other zones are limited to <200 ppm CRS (Fig. 5).

4.3. Sulfur isotopes

Total $\delta^{34}S$ values ($\delta^{34}S_{Total\text{-}S}$) were calculated by mass balance of the three separate sulfur fractions and range from −1.5 to 16.1‰ with an average of 6.4‰ (Table 4). Total sulfide $\delta^{34}S$ values ($\delta^{34}S_{sulfide}$), calculated as a mass balance of $\delta^{34}S_{AVS}$ and $\delta^{34}S_{CRS}$, range from −1.5 to 16.9‰ (Table 4). For the separate sulfur fractions, $\delta^{34}S_{AVS}$ ranges from −1.2 to 9.4‰, $\delta^{34}S_{CRS}$ from −3.9 to 25.3‰ and $\delta^{34}S_{sulfate}$ from −8.0 to 18.4‰ (Table 4). The general clustering of sulfide $\delta^{34}S$ values around $\delta^{34}S_{MORB}$ (0.1 ± 0.5‰; Sakai et al., 1984) accompanied by some enriched and depleted $\delta^{34}S$ values is similar to analyses from the upper ~500 m of Hole 735B (Fig. 6) (Alt and Anderson, 1991).

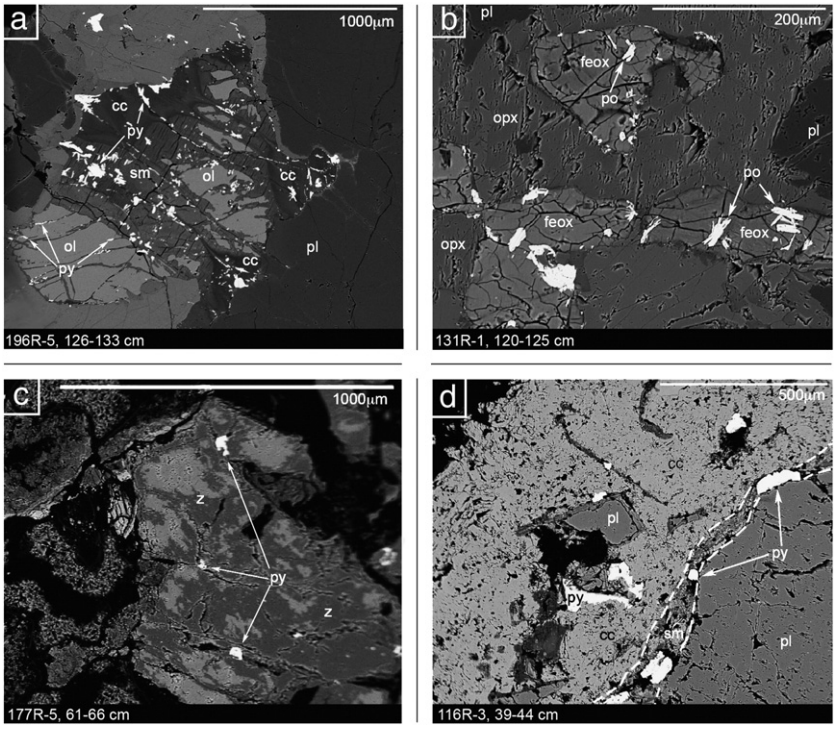

Fig. 3. BSE Images of common secondary sulfides in Hole 735B. **a.** Mesh texture of calcite and smectite hosting aggregate of pyrite laths among kernels of relict olivine. **b.** Pyrrhotite laths in iron-oxyhydroxide pseudomorphs of olivine. **c.** Blocky pyrite grains in smectite-lined fractures filled with zeolite. **d.** Pyrite grains in calcite vein and in smectite lining vein wall. Abbreviations: cc = calcite, feox = iron oxyhydroxide, ol = olivine, opx = orthopyroxene, pl = plagioclase, po = pyrrhotite, py = pyrite, sm = smectite, z = zeolites.

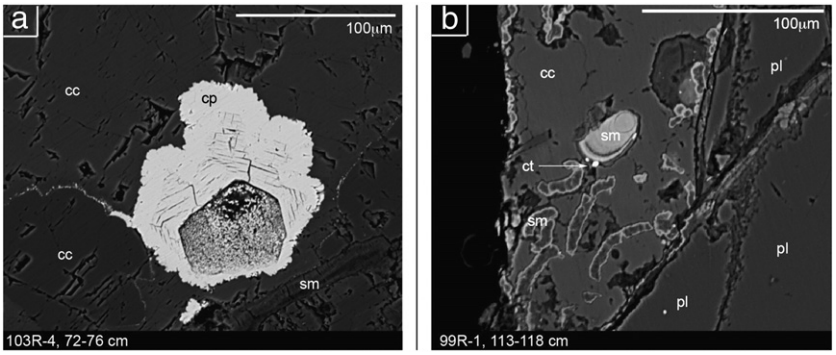

Fig. 4. BSE images of rare secondary sulfides in Hole 735B. **a.** Porous cauliflower chalcopyrite with shrinkage cracks in a blocky calcite vein lined with smectite. **b.** Globular chalcocite associated with vermicular smectite in a blocky calcite vein. cc = calcite, cp = chalcopyrite, ct = chalcocite, sm = smectite and pl = plagioclase.

5. Discussion

5.1. Sulfur changes during low temperature alteration

Samples from this study, specifically selected to reflect low temperature alteration effects, generally exhibit an increase in sulfur contents relative to unaltered rocks, but some samples show that sulfur has been lost locally. Bach et al. (2001) show that relatively unaltered samples from the lower 1000m of Hole 735B contain 100–1800 ppm S compared to 269–8305 ppm total S for our samples altered at low temperatures, indicating an overall addition of sulfur as the result of low temperature alteration. The majority of samples from this study have $SO_4/\Sigma S \leq 0.15$ (Table 4) and commonly host secondary sulfides. Two of the paired samples (116R-3, 39–44 cm and 127R-1, 105–109 cm) have higher sulfide contents and lower $SO_4/\Sigma S$ values in the highly altered sub-samples than in the associated minimally altered host rock sub-samples, consistent with an overall addition of sulfide during low-temperature alteration.

A few samples from this study provide evidence of significant local losses of sulfur during low-temperature alteration in alteration zone 1 in association with faults. Samples from the upper part of alteration zone 1 (96R-1, 36–40 cm and 99R-1, 113–118 cm) reflect a decrease in sulfur during low-temperature alteration: high $SO_4/\Sigma S$ values > 0.60 indicate more oxidizing conditions in this zone (Table 4). These rocks lack igneous sulfides, contain porous secondary sulfide grains, and have generally low sulfide-S contents (<120 ppm). These findings are consistent with the interpretation of Bach et al. (2001) for an oxidative loss of sulfur throughout alteration zone 1 by contact with relatively unreacted seawater associated with a large fault at 560 mbsf. Sulfur was lost locally elsewhere in the basement, as illustrated by the decrease in total sulfur (from 741 to 357 ppm) between the "minimally altered" and "highly altered" sub-samples of 133R-7, 107–111 cm (Table 4). Though this sample is within alteration zone 2, which is generally defined as a reductive zone (Bach et al., 2001), an increase in $SO_4/\Sigma S$ (from 0.06 to 0.46), decrease in sulfide sulfur (from 693 to 191 ppm), an increase in sulfate sulfur (from 48 to 166), and the presence of iron oxy-hydroxides

Table 4
Sulfur contents and isotopic compositions for whole-rock samples from the Leg 176 section of Hole 735B.

Lith. Unit	Alt. Zone	Core-Section, interval (cm)		Depth (mbsf)	S Contents (ppm)					$SO_4/\Sigma S$	$\delta^{34}S$ (‰)					
					AVS	CRS	Sulfide	Sulfate	Total*		AVS	CRS	Sulfide	Sulfate	Sulfate - Sulfide	Total**
VII		96R-1, 36–40		549.13	35	50	85	522	607	0.86	5.0	25.3	16.9	2.7	−14.2	4.7
VII	1	99R-1, 113–118		567.24	–	113	113	183	296	0.62		0.7	0.7	13.6	12.9	8.7
VIII		103R-4, 72–76		599.87	170	185	355	60	415	0.14	0.6	2.7	1.7	−1.9	−3.6	1.2
VIII		107R-1, 81–86		620.31	558	6576	7134	158	7292	0.02	8.7	16.9	16.3	9.0	−7.3	16.1
			Minimally altered	674.66	95	182	277	39	316	0.12	0.8	11.8	8.0	−4.8	−12.8	6.4
IX		116R-3, 39–44	Halo and pyrite vein		623	7564	8187	118	8305	0.01	8.4	9.8	9.7	2.0	−7.7	9.6
IX		118R-1, 8–14		690.88	555	1281	1836	68	1904	0.04	2.2	9.5	7.3	−1.2	−8.5	7.0
	2		Minimally altered	765.95	392	40	432	53	485	0.11	0.3	1.1	0.4	−0.9	−1.3	0.2
X		127R-1, 105–109	Halo		580	2316	2896	92	2988	0.03	9.4	8.2	8.4	−2.1	−10.5	8.1
X		131R-1, 120–125		804.70	997	520	1517	277	1794	0.15	6.7	5.5	6.3	3.9	−2.4	5.9
X		133R-7, 107–111	Minimally altered	832.33	684	9	693	48	741	0.06	4.4			−3.6		
			Halo		160	31	191	166	357	0.46	1.8	4.0	2.2	−5.6	−7.8	−1.4
X	3	140R-1, 119–124		881.49	321	39	360	58	418	0.14	−0.3	−3.9	−0.6	18.4	19.0	2.0
XI		150R-3, 56–62		973.12	253	13	266	8	274	0.03	1.1	−2.3	0.9	−0.9	−1.8	0.9
XI		159R-2, 74–80		1055.74	313	140	453	46	499	0.09	1.0	−2.3	0.0	−4.8	−4.8	−0.5
XI		168R-3, 59–64		1133.48	66	4978	5044	38	5082	0.01	−1.2	−1.5	−1.5	−8.0	−6.5	−1.5
XI	4	172R-7, 132–137		1178.13	1521	38	1559	138	1697	0.08	5.7	2.5	5.6	−4.3	−9.9	4.8
XI		177R-5, 61–66		1207.65	254	257	511				3.3	2.1	2.7			
XI		181R-2, 7–13		1241.70	6123	1425	7548	209	7757	0.03	5.4	4.7	5.3	3.9	−1.4	5.2
XII	5	196R-5, 126–132		1379.92	223	34	257	12	269	0.04	−0.8	−0.8	−0.8			
XII		202R-2, 135–141		1423.94	752	134	886	19	905	0.02	2.4	1.55	2.3	−5.7	−8.0	2.1

Lithologic units as presented by Dick et al., (1991) and Shipboard Scientific Party (1999).
Alteration Zones as defined by Bach et al. (2001).
– = none detected.
Blanks = not analyzed.
Total* = sum of extracted sulfur from AVS, CRS and Sulfate extractions.
Total** = ($\delta^{34}S_{AVS}$ x AVS Content/Σ S Content) + ($\delta^{34}S_{CRS}$ x CRS Content/Σ S Content) + ($\delta^{34}S_{SO4}$ x SO_4 Content/Σ S Content).
$SO_4/\Sigma S$ = (Sulfate S Content)/(Σ S Content).

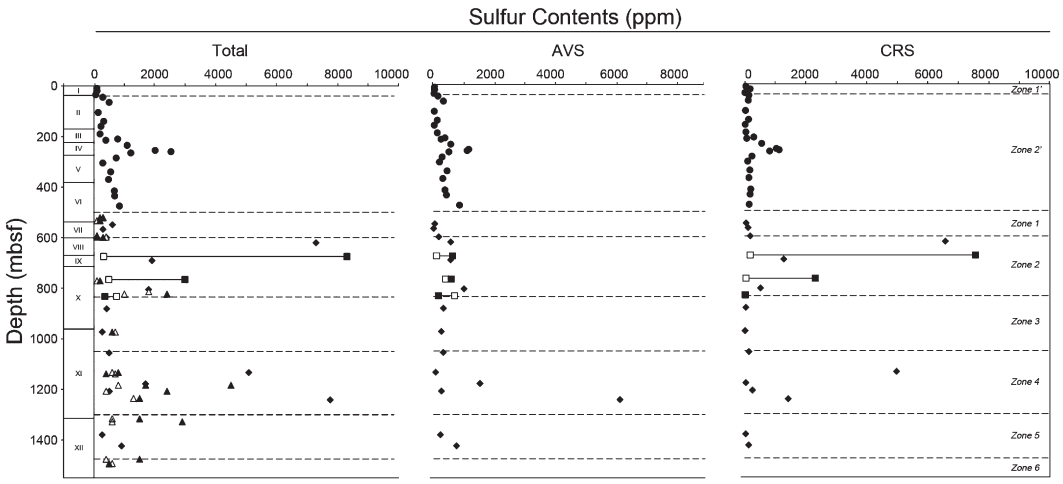

Fig. 5. Profile of total sulfur, AVS and CRS contents for whole-rock samples from Hole 735B. Filled circles (●) = Leg 118 samples from Alt and Anderson (1991) [Appendix 1], filled triangles (▲) = Leg 176 "altered" samples from Bach et al. (2001), open triangles (△) = Leg 176 "fresh" samples from Bach et al. (2001), filled diamonds (♦) = Leg 176 single samples from this study, filled squares (■) = Leg 176 "highly altered" sub-samples from this study, open squares (□) = Leg 176 "minimally altered" sub-samples from this study. Black solid tie-lines connect "altered" and "minimally altered" sub-sample pairs. Roman numerals denote lithologic stratigraphy as defined by Dick et al. (1991) and Shipboard Scientific Party (1999) [Table 1]. Dashed horizontal lines denote boundaries between low-temperature alteration zones as defined by Bach et al. (2001) [Table 2].

suggest an oxidative loss of sulfur during low-temperature alteration for this sample pair. Abundant smectites at this depth have been attributed to seawater infiltration through faults at 560 and 690 to 700 mbsf (Bach et al., 2001) and it is likely that these same faults may be responsible for the localized oxidation observed here. Oxidative processes throughout Hole 735B are further suggested by the $\delta^{34}S_{sulfate}$ values from this study which are all depleted in ^{34}S relative to seawater sulfate (Fig. 6). These relatively low values require a component of sulfate sulfur in Hole 735B that is sourced via oxidation of sulfides as precipitation does not impart fractionation upon the $^{34}S/^{32}S$ ratio of marine sulfate (Davis et al., 2003).

5.2. Microbial sulfate reduction

The secondary mineralogy and geochemistry of Hole 735B samples indicate sulfur addition in the form of sulfide minerals. The samples for this study host secondary smectite, carbonate, iron-oxyhydroxide and zeolite. Oxygen, strontium, and carbon isotope analyses of phyllosilicates and carbonates in these rocks indicate formation at temperatures less than 110 °C down to 10 °C, from 0 to 10 Ma seawater (Alt and Bach, 2001; Bach et al., 2001). Secondary phases in our samples are restricted to only those that form at low temperatures (<110 °C), so seawater sulfate is taken to be the source of sulfur added to the rocks, as opposed to sulfur derived from magmatic or high-temperature hydrothermal fluids.

Inorganic reduction of seawater sulfate and thermochemical sulfate reduction can be ruled out because these processes are kinetically inhibited at the low temperatures (<110 °C) prevailing for these samples, and at the moderate pH (~6) during seawater interaction with mafic rocks at these temperatures (Malinin and Khitarov, 1969; Seyfried and Bischoff, 1979; Ohmoto and Lasaga, 1982; Goldstein and Aizenshtat, 1994; Ohmoto and Goldhaber, 1997). Although there are viable chemical pathways by which thermochemical sulfate reduction

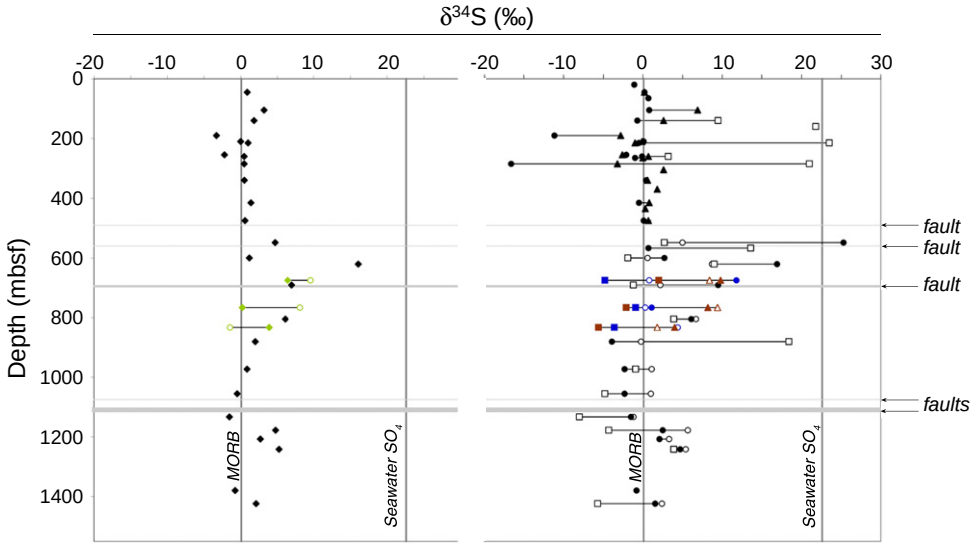

Fig. 6. Sulfur isotope profiles for Hole 735B whole-rock samples. Left: Profile of $\delta^{34}S_{Total}$ where black filled diamonds (♦) = "single sample", green filled diamonds (◆) = "minimally altered" sub-sample and open green diamond (◇) = "highly altered" sub-sample. Right: Profile of $\delta^{34}S$ by fraction where filled triangles (▲) = AVS, filled circles (●) = CRS, open squares (□) = sulfate, depth in meters below seafloor (mbsf). Black symbols are "single samples," brown symbols are "minimally altered" sub-samples and blue symbols are "highly altered" sub-samples. Solid black tie-lines connect fractions of the same whole-rock sample. After Sakai et al. (1984) and Davis et al. (2003) $\delta^{34}S$ reference lines are drawn at 0.1‰ for MORB and 22.6‰ for seawater sulfate. Values of samples from upper 500 m from Alt and Anderson (1991) [Appendix 1].

may operate at these temperatures, such processes require the presence of significant amounts of pre-existing H_2S and hydrocarbons to catalyze reduction reactions (Goldstein and Aizenshtat, 1994; Ohmoto and Goldhaber, 1997). Such conditions are present in oil-fields, where low-temperature thermochemical sulfate reduction has been proposed to take place, but are not consistent with sediment-free subseafloor basement environments as in the section penetrated by Hole 735B.

Microbial reduction of sulfate can occur from −1.5 to 110 °C (Jørgensen et al., 1992; Canfield, 2001), and is the only reasonable sulfate reducing mechanism to produce sulfide in the 10–110 °C temperature range indicated by our samples. Microbial sulfate reduction does not directly form iron-sulfide minerals but the signature of this process is recorded in the $\delta^{34}S$ of sulfide minerals. At equilibrium, SO_4 is enriched in ^{34}S relative to coexisting H_2S, and microbial sulfate reduction imparts a kinetic isotope fractionation primarily due to the biological preference for processing the weaker S–O bond formed with ^{32}S versus ^{34}S (Ohmoto and Goldhaber, 1997). The SO_4–H_2S isotope fractionation imparted by sulfate reducing bacteria can vary significantly due to temperature, rate of reduction, electron donor and the specific species of sulfate reducer involved, and has been described by enrichment factors of $\varepsilon_{SO4\text{-}H2S}$ up to 46‰ in natural samples (where $\varepsilon_{SO4\text{-}H2S} = \delta^{34}S_{SO4} - \delta^{34}S_{H2S}$) (Kaplan and Rittenberg, 1964; Canfield, 2001; Brunner and Bernasconi, 2005). Upon contact of H_2S with Fe^{2+} in solution, sulfide minerals readily precipitate with minimal fractionation of sulfur isotopes under the conditions of basement alteration and sulfate reduction in Hole 735B (Ohmoto and Rye, 1979; Ohmoto and Goldhaber, 1997).

Samples from this study have $\varepsilon_{SO4\text{-}sulfide}$ values ranging from 5.7 to 24.1‰ relative to $\delta^{34}S_{SO4}$ of 22.6‰ for seawater (Davis et al., 2003), which are generally consistent with isotope fractionation imposed by microbial sulfate reduction. Sulfur isotope data presented by Alt and Anderson (1991) for the uppermost 500 m of the core (Leg 118) have slightly larger $\varepsilon_{SO4\text{-}sulfide}$ values of 19.4 to 32.0‰. These data were previously interpreted in terms of high-temperature (~350 °C) hydrothermal processes and low-temperature oxidation plus disproportionation effects (Alt and Anderson, 1991). In light of our new data for samples affected only by low temperature processes, many of these older data containing sulfides in association with low-temperature alteration phases are better interpreted as the effects of microbial sulfate reduction. By comparison, serpentinites and marine sedimentary pyrites influenced by microbial sulfate reduction pathways display a range in $\varepsilon_{SO4\text{-}sulfide}$ of 21 to 66‰ and 24 to 71‰, respectively (Canfield and Teske, 1996; Alt and Shanks, 1998; Alt et al., 2007; Delacour et al., 2008b). Restriction to the lower end of viable enrichment factors in Hole 735B basement is due to a combination of potential factors: the involvement of different species of sulfate reducers, a greater utilization of H_2 in lieu of organic carbon as an electron donor, variable amounts of disproportionation of H_2S prior to iron sulfide precipitation, and reservoir effects (Kaplan and Rittenberg, 1964; Canfield, 2001).

5.2.1. Sulfate reduction pathways

Fig. 7 illustrates potential pathways for addition of microbial sulfide to Hole 735B gabbros. Unaltered gabbro is plotted at $\delta^{34}S_{sulfide} = 0.1$‰ (Sakai et al., 1984) and sulfide contents of 100–1800 ppm based on the range of sulfur contents for fresh gabbro samples from Leg 176 (Bach et al., 2001). Samples from this study and those of Alt and Anderson (1991) are variably enriched and depleted in $^{34}S_{sulfide}$ and sulfide-S relative to fresh gabbro. Values for $\varepsilon_{SO4\text{-}H2S}$ in natural populations of sulfate reducers generally range from 2 up to 46‰ (Kaplan and Rittenberg, 1964; Detmers et al., 2001) so lines in Fig. 7 illustrate addition of sulfide produced by open-system microbial reduction of seawater sulfate using these ε values and starting at varying initial sulfur contents for gabbro. Disproportionation of H_2S can result in greater isotope fractionation between sulfate and iron sulfide minerals, but the range of $\varepsilon_{SO4\text{-}H2S}$ in Fig. 7 is sufficient to

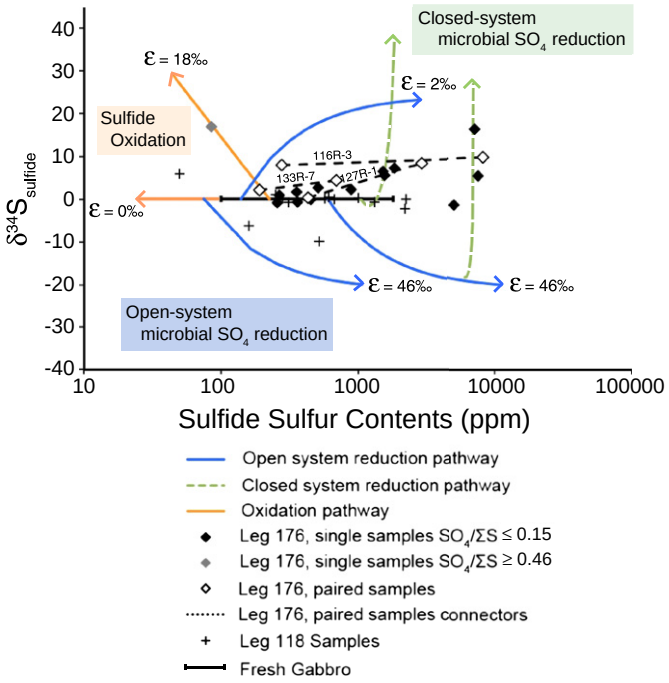

Fig. 7. Mechanisms affecting sulfur geochemistry of Hole 735B samples at low-temperature. Addition of sulfide to fresh gabbro (100–1800 ppm) through open-system reduction calculated based on $\varepsilon_{SO4\text{-}H2S} = 46$‰ and $\varepsilon_{SO4\text{-}H2S} = 2$‰ blue lines; (Kaplan and Rittenberg, 1964; Detmers et al., 2001), initial seawater sulfate $\delta^{34}S = 22.6$‰ (Davis et al., 2003) and a concentration of 28 mmol/kg (Pilson, 1988). Closed-system reduction pathways only shown for $\varepsilon_{SO4\text{-}H2S} = 46$‰ (green dashed lines) as the difference from closed-system reduction for $\varepsilon_{SO4\text{-}H2S} = 2$‰ is minimal. Loss of sulfide from fresh gabbro by oxidation calculated based on $\varepsilon_{H2S\text{-}SO4} = 0$‰ and $\varepsilon_{H2S\text{-}SO4} = 18$‰ (Ohmoto and Goldhaber, 1997; Canfield, 2001). Black diamonds (♦) = Leg 176 single-samples with $SO_4/\Sigma S < 0.16$, grey diamond (◆) = Leg single-sample with $SO_4/\Sigma S > 0.45$, open diamonds (◊) = Leg 176 paired highly and minimally altered sub-samples, and crosses (+) = Leg 118 samples. Capped black line (|—|) = range of unaltered gabbro from Hole 735B with $\delta^{34}S_{sulfide} = 0.1$‰ (Sakai et al., 1984) and sulfide sulfur contents = 100–1800 ppm (Bach et al., 2001).

illustrate processes in Hole 735B. Many samples fall along a rough trend of increasing S contents and increasing $\delta^{34}S$, and are consistent with sulfate reduction at low ε values, whereas the scattered negative $\delta^{34}S$ values are consistent with large values of ε. The area between the ε = 46‰ and ε = 2‰ lines illustrates that variations in ε can produce the observed elevated S contents of the gabbros at varying $\delta^{34}S$ values. In particular, negative $\delta^{34}S$ values at low S contents can be produced by open system sulfate reduction and addition of sulfide to the rock starting at lower initial S contents.

It is possible that reservoir effects may have influenced sulfur in our samples. The supply of dissolved sulfate to a specific location within the system may become limited, e.g., due to decreasing permeability or to sulfate reduction occurring upstream. Rayleigh fractionation processes would result in a progressive enrichment in ^{34}S of the dissolved sulfate reservoir as microbial sulfate reduction preferentially removes ^{32}S into H_2S. For an assumed seawater/rock ratio of 1, the amount of sulfur available would be a maximum of ~900 ppm (based on the concentration of dissolved sulfate available in seawater). The seawater/rock ratio for gabbros of the Atlantis Massif is generally low, however (Bach et al., 2001), so the concentration of sulfur available is likely much lower than 900 ppm, limiting the amount of S that could be added by this process. Thus, the effects of a closed system with reservoir effects on $\delta^{34}S$ are likely small, and are not distinguishable from the wide range of $\delta^{34}S_{sulfide}$ values that can be produced by microbial sulfate reduction in an open system in Hole 735B (Fig. 7).

5.3. Iron-silicate replacements and secondary sulfide precipitation

The presence of hematite lamellae in magnetite within olivine and clinopyroxene pseudomorphs of alteration zone 1 reflects oxic conditions, which led to loss of sulfur from rocks in this zone and prohibited formation of secondary sulfides. Oxygenated seawater was probably introduced through a permeable fault in the middle of this alteration zone at 560 mbsf (Dick et al., 2000). Continued reaction of these fluids with basement rocks would have eventually removed O_2 from solution, allowing for the establishment of obligate anaerobic microbial sulfate reducers down-flow from the fault, possibly deeper in the section.

The common presence of magnetite ($FeO \cdot Fe_2O_3$) in pseudomorphs of olivine and pyroxene, plus elevated Fe^{3+}/Fe^{total} measured by Bach et al. (2001) demonstrate localized oxidation of iron silicate minerals in Leg 176 samples altered at low temperatures. Oxidation of ferrous iron in olivine can produce H_2 through reduction of H_2O, which is common during serpentinization of seafloor peridotites and has been proposed for basalt-groundwater interaction (Alt and Shanks, 1998; Stevens and McKinley, 2000). As lithotrophic sulfate reducers utilize H_2 as an electron donor (Canfield, 2001; Edwards et al., 2005), the involvement of an H_2-forming reaction may have contributed to microbial activity, similar to mechanisms supporting autotrophic metabolisms in the Columbia River Basalts (Stevens and McKinley, 2000; Chapelle et al., 2002).

The lath morphology displayed by all secondary sulfides associated with olivine and clinopyroxene replacements suggests initial precipitation of these secondary sulfides as pyrrhotite. This would be expected regardless of sulfur fugacity due to the high nucleation barrier for pyrite with respect to monosulfides at temperatures less than 100 °C (Schoonen and Barnes, 1991). Transformation of pyrrhotite to pyrite to produce the observed pyrite laths can occur by addition of sulfur via sulfidation, or by Fe^{2+} loss through oxidation (Schoonen and Barnes, 1991; Belzile et al., 2004). Sulfidation is a possible mechanism for pyrite formation given the production of H_2S by sulfate reduction, but the distribution and textures of secondary minerals suggest otherwise. Less-altered host rocks contain well-crystallized pyrrhotite in pseudomorphs after olivine and pyroxene, and this grades to porous pyrrhotite and then lath-shaped pyrite in the highly altered wallrock adjacent to veins containing low-temperature alteration phases. This observed zonation is consistent with sulfidation in the formation of pyrrhotite, followed by an oxidation of pyrrhotite to pyrite. The oxidation of pyrrohtite to pyrite in alteration halos plus the greater concentration of sulfur in alteration halos relative to host rocks (Table 4: 127R, 105–109 cm and 116R-3, 39–44 cm) reflects greater initial sulfidation to pyrrhotite in the alteration halos compared to the adjacent host rock.

The lath morphology retained by the pyrite is not a characteristic morphology resulting from microbial oxidation of pyrrhotite (Bhatti et al., 1993), suggesting abiotic oxidation processes. Abiotic oxidation of pyrrhotite requires the presence of O_2 in solution (Knipe et al., 1995), which may have occurred locally within highly reacted areas as altering iron silicates became depleted in iron, thereby lowering the local reduction potential and allowing for incoming seawater to retain O_2 in solution longer. According to the experimental model by Pratt et al. (1994), progressive oxidation of pyrrhotite by O_2 would lead to the production of increasing Fe^{2+} deficiency in iron sulfides towards the main O_2 source, similar to the sulfide mineral gradients in wallrock adjacent to veins in Hole 735B. A similar Fe^{2+} deficiency in iron sulfides is also present with depth in the proportion of pyrite relative to pyrrhotite which decreases with depth, with abundant pyrite in zone 2, common pyrite in zone 3, and with pyrite generally absent in zones 4 and 5. Decreasing proportions of CRS compared to AVS with depth provide further evidence of this pattern (Fig. 5; Table 4) and reflects the progressive movement of the redox front through the system as the reduction potential of iron-silicates becomes exhausted. Though sulfur is also oxidized during the oxidation of pyrrhotite, the temporary formation of pyrite is allowable due to stoichiometric relationships which result in the oxidation of only 1 mol of sulfur for every 8 mol of iron that is oxidized (Bach and Edwards, 2003).

5.3.1. Oxidation pathways

Oxidation of sulfides in submarine environments can occur readily at low-temperatures via abiotic oxidation by dissolved oxygen (O_2) or by sulfide oxidizing microorganisms (Wirsen et al., 1993; Ohmoto and Goldhaber, 1997; Wirsen et al., 1998; Canfield, 2001). Abiotic oxidation of sulfide minerals is generally considered to result in little fractionation of sulfur isotopes (e.g., Taylor et al., 1984). Microbial oxidation of sulfide minerals has been shown to produce kinetic fractionation of sulfur isotopes because of the biological preference for processing ^{32}S (see Canfield, 2001). Values for $\varepsilon_{sulfate\text{-}sulfide}$ of up to −18‰ can occur from direct oxidation pathways, but some experiments show little or no fractionation during this process (e.g., Balci et al., 2007; Pisapia et al., 2007). Moreover, some experiments involving abiotic oxidation of sulfide minerals have shown a kinetic sulfur isotope fractionation of −0.7 to −3.8‰ (Balci et al., 2007; Thurston et al., 2010). Thurston et al. (2010) suggest that intermediate sulfur species (e.g., S°) are important in producing this kinetic isotope fractionation, and pH may be important. Thus, both abiotic and microbial oxidation of sulfide minerals can result in variable kinetic fractionation of sulfur isotopes, but this is not always the case. Values of $\varepsilon_{sulfate\text{-}sulfide}$ that might be expected during oxidation can thus range from 0‰ to −18‰.

Most samples from this study have $\delta^{34}S_{Sulfide}$ values greater than coexisting $\delta^{34}S_{SO4}$ (Table 4). This is opposite to the expected relationship at equilibrium, where species with higher oxidation states should have higher $\delta^{34}S$ values, and is consistent with kinetic isotope fractionation during oxidation of sulfide minerals. Sample 96R-1, 36–40 cm is highly oxidized ($SO_4/\Sigma S = 0.86$), has low sulfide contents (85 ppm), lacks secondary sulfides, contains rare porous igneous sulfides, and has a high $\delta^{34}S_{sulfide}$ value (16.9‰) (Fig. 7; Table 4). These points suggest kinetic fractionation of sulfur isotopes during oxidization of igneous sulfides, with loss of fractionated (^{32}S-enriched) sulfate resulting in enrichment of ^{34}S in the residual sulfide in the rock. The minimally altered portion of sample 116R-3, 39–44 cm lacks secondary sulfides, so the elevated $\delta^{34}S_{sulfide}$ value (8.0‰)

at low sulfur content (277 ppm sulfide-S) could reflect kinetic isotope effects during oxidation. Kinetic fractionation of sulfur isotopes during low-temperature oxidation of serpentinites and gabbros exposed at the seafloor has been documented elsewhere (Alt et al., 2007; Delacour et al., 2008a, 2008b).

In another paired sample, 133R-7, 107–111 cm, the less altered host rock portion has elevated $\delta^{34}S_{AVS}$ (4.4‰) at moderate sulfide-S contents (700 ppm), consistent with addition of microbial sulfide to the rock (Fig. 7, Table 4). The more highly altered part of this sample has low sulfur content and high $SO_4/\Sigma S$ (0.46) indicating loss of sulfur through oxidation. Negative $\delta^{34}S_{SO4}$–$\delta^{34}S_{Sulfide}$ for this sample indicates a kinetic isotope fractionation during oxidation, but the $\delta^{34}S_{sulfide}$ value of 2.2‰ does not reflect ^{34}S-enrichment compared to the host rock (4.4‰) that would be expected from this process. This may reflect isotopic heterogeneity in secondary sulfide added to the rocks prior to oxidation, or variable oxidation processes producing varying isotope fractionation during oxidation.

6. Summary and conclusions

The results of this study provide evidence for addition of sulfide to oceanic gabbros through microbial reduction of seawater sulfate. This shows that a subsurface microbial biosphere, identified in sediments and the uppermost basaltic layer of the oceanic crust, can also be present in the lower oceanic crust under appropriate low-temperature conditions.

Secondary sulfide minerals are common in gabbros of ODP Hole 735B affected by low-temperature (<110 °C) alteration. Laths of pyrrhotite and pyrite are present with smectite ± iron-oxyhydroxide ± magnetite ± calcite replacing olivine and clinopyroxene adjacent to veins of smectite ± calcite. Minor pyrite also occurs locally in veins of smectite ± calcite ± zeolite. Formation of secondary sulfides in altered gabbros led to gains of sulfur relative to fresh rocks (up to 7000–8000 ppm vs 100–1800 ppm, respectively). Because of the low temperatures of alteration, microbial reduction of seawater sulfate is the only viable mechanism for sulfide addition, and was likely enabled by the production of H_2 from the oxidation of ferrous iron in olivine and pyroxene. A wide range in $\delta^{34}S_{sulfide}$ values from −1.5 to 16.3‰ and variable additions of sulfide indicate that conditions ranged from open-system to closed-system with respect to seawater sulfate during microbial sulfate reduction.

Oxidation of sulfide minerals is evident in some highly oxidized samples that have low sulfur contents, high $SO_4/\Sigma S$ (≥0.46), contain porous igneous sulfides and globular secondary sulfides, and lack secondary sulfides. High $\delta^{34}S_{sulfide}$ values and negative $\varepsilon_{sulfate\text{-}sulfide}$ for some of these samples indicate a kinetic isotope effect during oxidation, which may be a biotic or abiotic process. Oxidation effects are likely related to seawater penetration along a permeable fault at 560 and 690–700 mbsf.

The amount of sulfide that was precipitated during low-temperature alteration may have been limited by the development of closed system reduction processes, and by local oxidation. Nonetheless, microbial interactions resulted in a net addition of sulfur to altered gabbros and an elevation of the average $\delta^{34}S_{Total}$ to 6.4‰ within local areas altered at temperature ≤110 °C. These results indicate that exposed lower oceanic crust can harbor measurable geochemical anomalies due to interactions with microorganisms, and that a subsurface biosphere can occur in the lower oceanic crust under appropriate conditions.

Supplementary materials related to this article can be found online at doi:10.1016/j.chemgeo.2011.05.005.

Acknowledgements

This research used samples provided by the Ocean Drilling Program (ODP) and Integrated Ocean Drilling Program (IODP), with financial support by the U.S. National Science Foundation (OCE-0622949). The authors thank Roland Thurston for analytical work. Wolfgang Bach and Adelie Delacour provided helpful reviews.

References

Alt, J.C., 2004. Alteration of the upper oceanic crust: mineralogy, chemistry, and processes. In: Davis, E.E., Elderfield, H. (Eds.), Hydrogeology of the Oceanic Lithosphere. Cambridge University Press, New York, pp. 497–595.

Alt, J.C., Anderson, T.F., 1991. Mineralogy and isotopic composition of sulfur in layer 3 gabbros from the Indian Ocean, Hole 735B. In: Von Herzen, R., Robinson, P.T., et al. (Eds.), Proc. ODP, Sci. Results, 118: College Station, TX (Ocean Drilling Program), pp. 113–125. doi:10.2973/odp.proc.sr.118.155.1991.

Alt, J.C., Bach, W., 2001. Data report: Low-grade hydrothermal alteration of uplifted lower oceanic crust, Hole 735B: mineralogy and isotope geochemistry. In: Natland, J.H., Dick, H.H.R., Miller, D.J., Von Herzen, R.P. (Eds.), Proc. EDP, Sci Results, 176, pp. 1–24.

Alt, J.C., Bach, W., 2006. Oxygen isotope composition of a section of lower oceanic crust, ODP Hole 735B. Geochem. Geophy. Geosyst. 7, Q12008. doi:10.1029/2006GC001385.

Alt, J.C., Shanks, W.C., 1998. Sulfur in serpentinized oceanic peridotites: serpentinization processes and microbial sulfate reduction. J. Geophys. Res. 103, 9917–9929.

Alt, J.C., Shanks, W.C., 2003. Serpentinization of abyssal peridotites from the MARK area. Mid-Atlantic Ridge: Sulfur geochemistry and reaction modeling. Geochim. Cosmochim. Acta 67, 641–653.

Alt, J.C., Davidson, G.J., Teagle, D.A.H., Karson, J.A., 2003. Isotopic composition of gypsum in the Macquarie Island ophiolite: Implications for the sulfur cycle and the subsurface biosphere in oceanic crust. Geology 31, 549–552.

Alt, J.C., Shanks, W.C., Bach, W., Paulick, H., Garrido, C.J., Beaudoin, G., 2007. Hydrothermal alteration and microbial sulfate reduction in peridotite and gabbro exposed by detachment faulting at the Mid-Atlantic Ridge, 15°20'N (ODP Leg 209): A sulfur and oxygen isotope study. Geochem. Geophy. Geosyst. 8, Q08002. doi:10.1029/2007GC001617.

Bach, W., Edwards, K.J., 2003. Iron and sulfide oxidation within the basaltic ocean crust: Implications for chemolithoautotrophic microbial biomass production. Geochim. Cosmochim. Acta 67 (20), 3871–3887. doi:10.1016/S0016-7037(03)00304-1.

Bach, W., Alt, J.C., Niu, Y.L., Humphris, S.E., Erzinger, J., Dick, H.J.B., 2001. The geochemical consequences of late-stage low-grade alteration of lower ocean crust at the SW Indian Ridge: Results from ODP Hole 735B (Leg 176). Geochim. Cosmochim. Acta 65, 3267–3287.

Balci, N., Shanks, W.C., Mayer, B., Mandermack, K.W., 2007. Oxygen and sulfur isotope systematics of sulfate produced by bacterial and abiotic oxidation of pyrite. Geochim. Cosmochim. Acta 71, 3796–3811.

Beaudoin, G., Taylor, B.E., Rumble, D., Thiemens, M., 1994. Variations in the sulfur isotope composition of troilite for the Canon-Diablo iron meteorite. Geochim. Cosmochim. Acta 58, 4253–4255.

Belzile, N., Chen, Y.W., Cai, M.F., Li, Y.R., 2004. A review on pyrrhotite oxidation. J. Geochem. Explor. 84, 65–76.

Bhatti, T.M., Bigham, J.M., Carlson, L., Tuovinen, O.H., 1993. Mineral Production of Pyrrhotite Oxidation by *Thiobacillus ferrooxidans*. Appl. Environ. Microbiol. 59, 1984–1990.

Boschi, C., Dini, A., Früh-Green, G.L., Kelley, D.S., 2008. Isotopic and element exchange during serprentinization and metasomatism at the Atlantis Massif (MAR 30°N): Insights from B and Sr isotope data. Geochim. et Cosmochim. Acta 72, 1801–1823.

Brunner, B., Bernasconi, S.M., 2005. A revised isotope fractionation model for dissimilatory sulfate reduction in sulfate reducing bacteria. Geochim. et Cosmochim. Acta 69, 4759–4771.

Buck, W.R., Lavier, L.L., Paliakov, A.N.B., 2005. Modes of faulting at mid-ocean ridges. Nature 434, 719–723.

Canfield, D.E., 2001. Biogeochemistry of sulfur isotopes. In: Valley, J.W., Cole, D.R. (Eds.), Reviews in Mineralogy and Geochemistry: The Mineralogical Society of America, Blacksburg, 43, pp. 607–636.

Canfield, D.E., Teske, A., 1996. Late Proterozoic rise in atmospheric oxygen concentration inferred from phylogenetic and sulphur-isotope studies. Nature 54, 127–132.

Canfield, D.E., Raiswell, R., Westrich, J.T., Reaves, C.M., Berner, R.A., 1986. The use of chromium reduction in the analysis of reduced inorganic sulfur in sediments and shales. Chem. Geol. 54, 149–155.

Carbotte, S.M., Scheirer, D.S., 2004. Variability of ocean crustal structure created along the global mid-ocean ridge. In: Davis, E.E., Elderfield, H. (Eds.), Hydrogeology of the Oceanic Lithosphere. Cambridge University Press, New York, pp. 59–106.

Chapelle, F.H., O'Neill, K., Bradley, P.M., Methe, B.A., Ciufo, S.A., Knobel, L.L., Lovely, D.R., 2002. A hydrogen-based subsurface microbial community dominated by methanogens. Nature 415, 312–314.

Coplen, T.B., Krouse, H.R., 1998. Sulphur isotope data consistency improved. Nature 392, 32.

Cowen, J.P., Giovannoni, S.J., Kenig, F., Johnson, H.P., Butterfield, D., Rappe, M.S., Hutnak, J., Lam, P., 2003. Fluids from aging ocean crust that support microbial life. Science 299, 120–123.

Davis, A.S., Clague, D.A., Zierenberg, R.A., Wheat, C.G., Cousens, B.L., 2003. Sulfide formation related to changes in the hydrothermal system on Loihi Seamount, Hawai'I, following the seismic event in 1996. Can. Mineral. 41, 457–472.

Delacour, A., Fruh-Green, G.L., Bernasconi, S.M., Kelley, D.S., 2008a. Sulfur in peridotites and gabbros at Lost City (30°N, MAR): Implications for hydrothermal alteration and microbial activity during serpentinization. Geochim. Cosmochim. Acta 72, 5090–5110.

Delacour, A., Früh-Green, G.L., Bernasconi, S.M., 2008b. Sulfur mineralogy and geochemistry of serpentinites and gabbros of the Atlantis Massif (IODP Site U1309). Geochim. Cosmochim. Acta 72, 5111–5127.
Detmers, J., Brüchert, V., Habicht, K.S., Kuever, J., 2001. Diversity of sulfur isotope fractionations by sulfate-reducing prokaryotes. Appl. Environ. Microbiol. 67, 888–894.
Dick, H.J.B., Meyer, P.S., Bloomer, S., Kirby, S., Stakes, D., Mawer, C., 1991. Lithostratigraphic evolution of an in-situ section of oceanic layer 3. In: Von Herzen, R., Robinson, P.T., et al. (Eds.), Proc. ODP, Sci. Results, 118: College Station, TX (Ocean Drilling Program), pp. 439–538. doi:10.2973/odp.proc.sr.118.128.1991.
Dick, H.J.B., Natland, J.H., Alt, J.C., Bach, W., Bideau, D., Gee, J.S., Haggas, S., Hertogen, J.G.H., Hirth, G., Holm, P.M., Ildefonse, B., Iturrino, G.J., John, B.E., Kelley, D.S., Kikawa, E., Robinson, P.T., Snow, J., Stephen, R.A., Trimby, P.W., Worm, H.U., Yoshinobu, A., 2000. A long in-situ section of the lower ocean crust: results of ODP Leg 176 drilling at the Southwest Indian Ridge. Earth Planet Sci. Lett. 179, 31–51.
Edmond, J.M., Measures, C., McDuff, R.E., Chan, L.H., Collier, R., Grant, B., Gordon, L.I., Corliss, J.B., 1979a. Ridge crest hydrothermal activity and the balances for the major and minor elements in the ocean – Galapagos data. Earth Planet Sci. Lett. 46, 1–18.
Edmond, J.M., Measures, C., Measures, C., Mangum, B., Grant, B., Sclater, F.R., Collier, R., Hudson, A., Gordon, L.I., Corliss, J.B., 1979b. Formation of metal-rich deposits at ridge crests. Earth Planet Sci. Lett. 46, 19–30.
Edwards, K.J., Bach, W., McCollom, T.M., Rogers, D.R., 2004. Neutrophilic Iron-Oxidizing Bacteria in the Ocean: Their Habitats, Diversity and Roles in Mineral Deposition, Rock Alteration and Biomass Production in the Deep Sea. Geomicrobiol. J. 21, 393–404. doi:10.1080/01490450490485863.
Edwards, K.J., Bach, W., McCollom, T.M., 2005. Geomicrobiology in oceanography: microbe-mineral interactions at and below the seafloor. Trends Microbiol. 13, 449–456. doi:10.1016/j.tim.2005.07.005.
Escartin, J., Mével, C., MacLeod, C.J., McCaig, A.M., 2003. Constraints on deformation conditions and the origin of oceanic detachments: The Mid-Atlantic Ridge core complex at 15°45'N. Geochem. Geophy. Geosyst. 4. doi:10.1029/2002GC000472.
Fisher, A.T., 1998. Permeability within basaltic oceanic crust. Rev. Geophys. 36, 143–182.
Fisk, M.R., Giovannoni, S.J., Thorseth, I.H., 1998. Alteration of oceanic volcanic glass: Textural evidence of microbial activity. Science 281, 978–980.
Furnes, H., Staudigel, H., 1999. Biological mediation in ocean crust alteration: how deep is the deep biosphere? Earth Planet Sci. Lett. 166, 97–103.
Goldstein, T.P., Aizenshtat, Z., 1994. Thermochemical sulfate reduction – A review. J. Therm. Anal. 42, 241–290.
Honnorez, J., 2003. Hydrothermal alteration vs. ocean-floor metamorphism. A comparison between two case histories: the TAG hydrothermal mound (Mid-Atlantic Ridge) vs. DSDP/ODP Hole 504B (Equatorial East Pacific). C.R. Geoscience 335, 781–824.
Huber, J.A., Johnson, H.P., Butterfield, D.A., Baross, J.A., 2006. Microbial life in ridge flank crustal fluids. Eviron. Microbiol. 8, 88–99.
Hutnak, M., Fisher, A.T., Harris, R., Stein, C., Wang, K., Spinelli, G., Schindler, M., Villinger, H., Silver, E., 2008. Large heat and fluid fluxes driven through mid-plate outcrops on ocean crust. Nat. Geosci. 1, 611–614. doi:10.1038/ngeo264.
Ildefonse, B., Blackman, D.K., John, B.E., Ohara, Y., Miller, D.J., MacLeod, C.J., 2007. Oceanic core complexes and crustal accretion at slow-spreading ridges. Geology 35, 623–626.
John, B.E., Foster, D.A., Murphy, J.M., Cheadle, M.J., Baines, A.G., Fanning, C.M., Copeland, P., 2004. Determining the cooling history of in situ lower oceanic crust – Atlantis Bank, SW Indian Ridge. Earth Planet Sci. Lett. 222, 145–160.
Jørgensen, B.B., Isaksen, M.F., Jannasch, H.W., 1992. Bacterial sulfate reduction above 100-degrees-C in deep-sea hydrothermal vent sediments. Science 258, 1756–1757.
Kaplan, I.R., Rittenberg, S.C., 1964. Microbiological fractionation of sulphur isotopes. Microbiology 34, 195–212.
Karson, J.A., 1998. Geological investigation of a lineated massif at the Kane Transform Fault: implications for oceanic core complexes. Phil. Trans.: Math. Phys. Eng. Sci. 357, 713–740.
Kelley, D.S., Baross, J.A., Delaney, J.R., 2002. Volcanoes, Fluids, and Life at Mid-Ocean Ridge Spreading Centers. Annu. Rev. Earth Planet Sci. 30, 385–491. doi:10.1146/annurev.earth30.091201.141331.
Knipe, S.W., Mycroft, J.R., Pratt, A.R., Nesbitt, H.W., Bancroft, G.M., 1995. X-ray photoelectron spectroscopic study of water-adsorption on iron sulfide minerals. Geochim. Cosmochim. Acta 59, 1079–1090.
Malinin, S.D., Khitarov, N.I., 1969. Reduction of sulfate sulfur by hydrogen under hydrothermal conditions. Geochem. Int. Ussr 6, 1022–1027.
Miller, D.J., Cervantes, P., 2002. Sulfide mineral chemistry and petrography and platinum group element composition in gabbroic rocks from the Southwest Indian Ridge. In: Natland, J.H., Dick, H.J.B., Miller, D.J., Von Herzen, R.P. (Eds.), Proc. ODP, Sci. Results, 176, pp. 1–29. doi:10.2973/odp.proc.sr.176.009.2002.
Natland, J.H., Dick, H.J.B., Miller, D.J., Von Herzen, R.P. (Eds.), 2002. Proc. ODP, Sci. Results, 176: College Station, TX (Ocean Drilling Program). doi:10.2973/odp.proc.sr.176.2002.
Ohmoto, H., Goldhaber, M.B., 1997. Suflur and Carbon Isotopes. In: Hubert, L.B. (Ed.), Geochemistry of Hydrothermal Deposits. Wiley & Sons, New York, pp. 517–612.
Ohmoto, H., Lasaga, A.C., 1982. Kinetics of reactions between aqueous sulfates and sulfides in hydrothermal systems. Geochim. Cosmochim. Acta 46, 1727–1745.
Ohmoto, H., Rye, R.O., 1979. Isotopes of sulfur and carbon. In: Barnes, H.L. (Ed.), Geochemistry of Hydrothermal Ore Deposits. Wiley & Sons, New York, pp. 509–567.
Pilson, M.Q., 1988. An Introduction to the Chemistry of the Sea. Prentice Hall, Upper Saddle River.
Pisapia, C., Chaussidon, M., Mustin, C., Humbert, B., 2007. O and S isotopic composition of dissolved and attached oxidation products of pyrite by *Acidithiobacillus ferrooxidans*: Comparison with abiotic oxidation. Geochim. et Cosmochim Acta 71, 2474–2490.
Pratt, A.R., Muir, I.J., Nesbitt, H.W., 1994. X-ray photoelectron and Auger electron spectroscopic studies of pyrrhotite and mechanism of air oxidation. Geochim. et Cosmochim. Acta 58, 827–841.
Rice, C.A., Tuttle, M.L., Reynolds, R.L., 1993. The analysis of forms of sulfur in ancient sediments and sedimentary rocks – Comments and cautions. Chem. Geol. 107, 83–95.
Rouxel, O., Ono, S.H., Alt, J., Rumble, D., Ludden, J., 2008. Sulfur isotope evidence for microbial sulfate reduction in altered oceanic basalts at ODP Site 801. Earth Planet Sci. Lett. 268, 11–123. doi:10.1016/j.epsl.2008.01.010.
Sakai, H., Desmarais, D.J., Ueda, A., Moore, J.G., 1984. Concentrations and isotope ratios of carbon, nitrogen and sulfur in ocean-floor basalts. Geochim. Cosmochim. Acta 48, 2433–2441.
Schoonen, M.A.A., Barnes, H.L., 1991. Reactions forming pyrite and marcasite from solutions. 2. Via FeS precursors below 100-degrees-C. Geochim. Cosmochim. Acta 55, 1505–1514.
Seyfried, W.E., Bischoff, J.L., 1979. Low temperature basalt alteration by seawater: an experimental study at 70 °C and 150 °C. Geochim. Cosmochim. Acta 43, 1937–1947.
Shilobreeva, S., Martinez, I., Busigny, V., Agrinier, P., Laverne, C., 2011. Insights into C and H storage in the altered oceanic crust: Results from ODP/IODP Hole 1256D. Geochim. et Cosmochim Acta 75, 2237–2255. doi:10.1016/g.gca.2010.11.027.
Shipboard Scientific Party, 1999. Leg 176 summary. In: Dick, H.J.B., Natland, J.H., Miller, D.J., et al. (Eds.), Proc. ODP, Init. Repts., 176: College Station, TX (Ocean Drilling Program), pp. 1–70. doi:10.2973/odp.proc.ir.176.101.1999.
Stevens, T.O., McKinley, J.P., 2000. Abiotic controls on H_2 production from basalt-water reactions and implications for aquifer biogeochemistry. Environ. Sci. Technol. 34, 826–831.
Taylor, B.E., Wheeler, M.C., Nordstrom, D.K., 1984. Isotope composition of sulphate in acid mine drainage as measure of bacterial oxidation. Nature 308, 538–540.
Thode, H.G., Monster, J., Dunford, H.B., 1961. Sulfur isotope geochemistry. Geochim. Cosmochim. Acta 25, 159–174.
Thurston, R.S., Mandemack, K.W., Shanks, W.C., 2010. Laboratory chalcopyrite oxidation by *Acidithiobacillus ferrooxidans*: Oxygen and sulfur isotope fractionation. Chem. Geol. 269, 252–261.
Torsvik, T., Furnes, H., Muehlenbachs, K., Thorseth, I.H., Tumyr, O., 1998. Evidence for microbial activity at the glass-alteration interface in oceanic basalts. Earth Planet Sci. Lett. 162, 165–176.
Tucholke, B.E., Lin, J., Kleinrock, M.C., 1998. Megamullions and mullion structure defining oceanic metamorphic core complexes on the Mid-Atlantic Ridge. J. Geophys. Res. 103, 9857–9866.
Tuttle, M.L., Goldhaber, M.B., Williamson, D.L., 1986. An analytical scheme for determining forms of sulfur in oil shales and associated rocks. Talanta 33, 953–961.
Wheat, C.G., Mottl, M.J., 2000. Composition of pore and spring waters from Baby Bare: global implications geochemical fluxes from a ridge flank hydrothermal system. Geochim. Cosmochim. Acta 64, 629–642.
Wirsen, Co, Jannashc, H.W., Molyneaux, S.J., 1993. Chemosynthetic microbial activity at Mid-Atlantic Ridge hydrothermal vent sites. J. Geophys. Res.-Solid Earth 98, 9693–9703.
Wirsen, C.O., Brinkhoff, T., Kuever, J., Muyzer, G., Molyneaux, S., Jannasch, H.W., 1998. Comparison of a new *Thiomicrospira* strain from the Mid-Atlantic Ridge with known hydrothermal vent isolates. Appl. Environ. Micro. 64, 4057–4059.
Zhabina, N.N., Volkov, I.I., 1978. A method of determination of various sulfur compounds in sea sediments and rocks. In: Krumbein, W.E. (Ed.), Environmental Biogeochemistry and Geomicrobiology. Ann Arbor Science, Ann Arbor MI, pp. 735–746.
Zindler, A., Hart, S., 1986. Chemical Geodynamics. Annu. Rev. Earth Planet Sci. 14, 493–571.